International Journal of Concrete Structures and Materials
Vol.19, No.1E, pp.33~39, March 2007

Finite Element Analysis on Hydration Heat of Concrete under the Influence of Reinforcing Steel Bars

Dong-Yong Yoon[1], Hyung-Soo Song[2], and Chang-Shik Min[3]

(Originally published in Korean version of ***Journal of KCI***, Vol.17, No.1, February 2005)

Abstract: The magnitude and distribution of hydration heat of concrete structures are related to the thermal properties of each component of the concrete, the initial temperature, the type of formwork, and the ambient temperature of exposed surfaces. Even though the reinforcing steel bar has completely different thermal properties, it has been excluded in the thermal analysis of the concrete structures for uncertain reasons. In this study, finite element analysis was performed on the concrete structures reinforced with steel bars in order to investigate the effect of reinforcing steel bars on the temperature and stress distribution due to the heat of hydration. As the steel content increased, the maximum temperature and the difference in the internal-external temperature decreased by 32.5% and 10.0%, respectively. It is clearly shown that the consideration of the influence of reinforcing steel bars in the heat of hydration analysis is necessary to obtain realistic solutions for the prediction of the maximum temperature and stresses of concrete structures.

Keywords: finite element analysis, heat of hydration, steel ratio, thermal property

1. Introduction

Concrete is subject to huge heat of hydration when it undergoes hydration process. Nevertheless, because the concrete structures with thin surface exposed to air can transmit the heat of hydration from inside to outside easily, it is not so much of concern. However, mass concrete structures are subject to large difference in temperature between the inside and the surface to release the heat of hydration, and thermal change creates a change in the volume. When this volumetric change is confined, confinement stress occurs by the principle as illustrated in Fig. 1. This deformation confinement affects the size and thermal stress occurrence of mass concrete structures greatly. Since thermal stress due to hydration heat can cause a severe crack in the structure, it is very important to predict the transmission of the hydration heat and its distribution accurately.

The factors of influence on the hydration heat are type of cement, temperature during concrete placement, type of admixtures, thermal property of concrete (thermal conductivity, specific heat, density, caloric value), etc. The most important component which determines the thermal property of concrete is the characteristics of the aggregate. Nonetheless, the total amount of steel bars reinforcing the steel concrete structure is too huge to be ignored, and the thermal property of the steel bar also shows a big difference with the concrete. Especially, the thermal conductivity of the steel bar is about 30~60 times that of concrete, and it affects the speed of heat conduction. Moreover, the steel bars exposed to the outside for the connectivity during construction can carry out the function of pipe cooling. Thus, it is expected that it can reduce the maximum temperature inside the structure due to the heat of hydration. Nevertheless, the research on the influence of steel bars in terms of hydration heat transfer and thermal stress is inadequate as of yet. Previous research of Kang, S. H. et al.[1] and the finite element analysis of Kim, E. G. et al.,[2] Kim, J. G. et al.[3,4] and Oh, B. H. et al.[5] focused on the material aspect of concrete and aggregate, etc. as well as the effective prediction of pipe cooling and the development of effective elements, etc. When carrying out the thermal analysis of concrete, it is possible to take the steel bar ratio into account for thermal property values. However, it is more desirable to conduct the analysis by considering the steel bar and concrete separately for more accurate prediction, because the steel bar is placed in specific locations and not uniformly distributed throughout the structure.

Thus, this study investigated this matter with emphasis on how the rebars inside the structure affects the dispersion of the hydration heat and the distribution of temperature as well as the thermal stress caused by it. The usual finite element analysis program[7] was used as an analysis tool, and an actual bridge pier was modelled for the analysis. Finally, we investigated the possibility of reducing the quantity of thermal rebars, which are placed for the purpose of temperature control, based on the analysis result.

2. Distribution of hydration heat and thermal stress property

2.1 Factors of influence on the distribution of heat of hydration

The heat of hydration is caused by the flow of heat between

[1] KCI member, Hyundai Steel Co., Seoul 137-938, Korea.
[2] KCI member, Dept. of Civil & Environmental Engineering, Dongguk University, Seoul 100-715, Korea.
[3] KCI member, Dept. of Civil & Environmental Engineering, Dongguk University, Seoul 100-715, Korea. *E-mail: csmin@dongguk.edu*

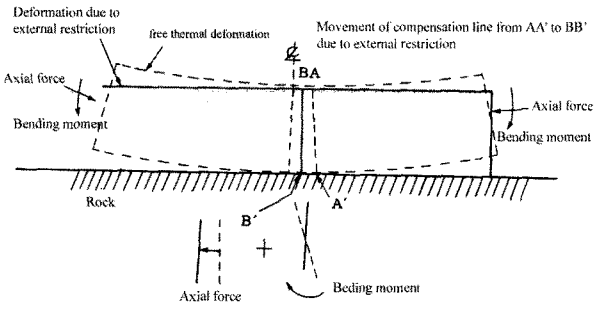

Fig. 1 Deformation due to external restriction.[7]

heat conduction inside the concrete and other materials. This heat flow is influenced by thermal conductivity of the concrete, specific heat, heat convectivity, etc. The thermal conductivity of concrete shows a distribution of 2.2~2.4 kcal/mhr°C, and it is determined by the property of materials composing the concrete. It can be expressed as the weighted average value of multiplying each material property value by the mass (weight) ratio. The specific heat, which indicates the amount of heat calorie required to change the temperature by one unit temperature per unit mass, shows increasing tendency with the water content of the concrete and the temperature increase. The specific heat of concrete is typically within the range of 0.25~0.3 kcal/kg°C.

Heat convectivity is a value indicating the characteristics of heat flow between the concrete structure and atmospheric air. Thus, the heat convectivity of concrete is influenced greatly by the heat distribution on its surface and also by water content of the concrete. The concrete is influenced by such numerous factors as solar radiation, water evaporation, latent heat, wind, spraying of water for wet curing, thermal insulation materials, etc in the field. However, because these factors change by each moment, it is difficult to delineate their influence accurately. Thus, under the assumption that the curing condition during concrete placement does not change at a given construction site, the heat convectivity under the environmental conditions of each site is regarded as the unique thermal property of the site. Generally, only the average wind velocity and artificial curing conditions are considered.

The thermal properties of the concrete and base rock applied in this study used the values cited from Kim, E. G et. al.,[2] and the thermal property of the rebars cited the values specified in Concrete Standard Specifications.[6] Table 1 summarizes thermal properties of materials used in this analytic study.

2.2 Factors of influence on thermal stress

The principle of thermal stress is that, as the rise in temperature inside the concrete due to heat of hydration and the drop in temperature due to the release of the heat to outside occurs simultaneously as in Fig. 1, volume changes occur at every location, but these force for volumetric change are confined by the foundation plate or already placed concrete to bring about a confinement stress. This confinement stress is determined by confinement strain and coefficient of elasticity, and its magnitude varies by the location of the cross section. Although coefficient of elasticity is a function of time, this study fixed it as a constant value due to the limitation of the analysis program module. Additionally, the volume change is determined by the coefficient of heat expansion and the magnitude of temperature change, and the coefficient of heat expansion for the cement paste and aggregate as the main compositional materials is different from each other. Typically, the coefficient of heat expansion for the cement paste and aggregate has the value of $10\sim20\times10^{-6}/°C$ and $6\sim12\times10^{-6}/°C$, respectively. Table 2 summarizes the dynamic (mechanical) properties of the concrete being applied in this study.

Generally, the loading condition in heat analysis problems is represented by the heat calorie stored inside and inflow of the heat from the outside due to convection. This study considered only these loading conditions, i.e. the heat of hydration generated from the inside and the heat convectivity released from the structural surface to the outside air, and ignored the condition of reflection heat energy.

2.3 Adiabatic temperature rising equation

An equation to predict the change in heat of hydration with time is called an adiabatic temperature rising equation, and the method to compute this heat variation is a very important in heat analysis. The adiabatic temperature rising equation as specified by Concrete Standard Specifications[6] is expressed as follows.

$$T = K(1 - e^{-\alpha t}) \quad (1)$$

where, t is the age (days), K is the magnitude of adiabatic temperature rising at the end, and α is the speed of temperature rising. This study applied $K = 45.5°C$ and $\alpha = 0.86$ as determined by the adiabatic temperature rising experiment of Kim, E. G et al.[2] The heat of hydration inside the concrete can be calculated by taking the differential of the heat of hydration computed by eq. (1) with respect to the time and then multiplying it by heat calorie per volume ($\rho_c C_c$). Thus, the heat of hydration generated inside

Table 1 Thermal properties of materials.

Property	Thermal conductivity (kJ/mhr°C)	Specific heat (kJ/m³°C)	Heat convectivity (kJ/m²hr°C)		Unit weight (N/m³)
Concrete	8.14	2,058.3	Surface	50.21	23,000
			Form	20.92	
Base rock	8.12	2,719.6	-		26,000
Steel	242.5	3,619.8	1,372.4		75,000

Table 2 Mechanical properties of materials.

Properties	Compressive strength (MPa)	Young's modulus (MPa)	Coefficient of expansion (/°C)	Poisson's ratio
Value	25	2.3 × 104	10×10^{-6}	0.167

the concrete can be expressed by the following equation.

$$q = \frac{\rho_c C_c \Delta T}{\Delta T} = \frac{1}{24}\rho_c C_c \alpha K e^{-\frac{\alpha t}{24}} \quad (2)$$

where, ρ_c : density of concrete
C_c : specific heat of concrete

Fig. 2 illustrates the floating of the heat of hydration inside the concrete from the adiabatic temperature rising equation of this study with respect to time.

3. Finite element analysis

3.1 Overview of finite element analysis

This study carried out analyses of heat of hydration and the heat stress caused by it with a general-purpose structural analysis program, ADINA.[7] The analysis process started with the analysis of heat (temperature) distribution in accordance with the time passage, and then the result of the heat analysis was used as the input for the load (heat stress) to carry out an analysis of the stress again. The finite element analysis program used in this study uses the following equilibrium equation for the heat flow.

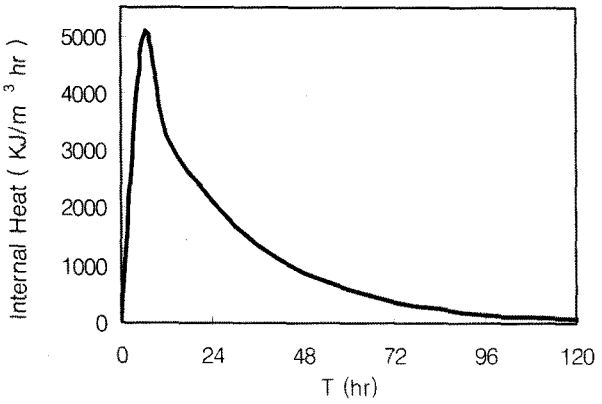

Fig. 2 Internal heat generation.

$$[C]\left\{\frac{\partial T}{\partial t}\right\} + [K]\{t\} = \{Q\} \quad (3)$$

where, [C] : heat calorie matrix
[K] : heat conduction matrix
{Q} : thermal (heat, temperature) load vector

Additionally, ADINA[7] uses Euler's backward integration and transient analysis methods in order to obtain the solution to the above equation.

3.2 Structures subjected to the analysis

3.2.1 Model

The bridge foundation at xxx bridge in xth construction section on Nohn~Dangjin expressway was chosen as the model used for this analysis. This model is a typical structure constructed and found in many bridge pier. Figs. 3 and 4 illustrate the diagram of the reinforcing steel bars embedded in the bridge pier subjected to the analysis of this study.

3.2.2 Steel ratio and computation of two-dimensional conversion thickness

This study varied the ratio of the reinforcing steel bars by 0%, 1.4%, 1.6%, and 1.8% in order to investigate the pattern of the distribution of heat of hydration by the ratio of the reinforcing steel bars with the application of finite element analysis method (FEM). The ratio of the steel bar volume to the concrete volume (hereinafter, steel bar ratio) used in the foundation of the subject structure was selected as the only variable of the analysis, and all the other conditions were fixed. All volumes of the steel bars including not only the main steel bars at the foundation but also compressed steel bars, stirrups, steel bars at the axial direction of the column, tie steel bars, etc. were considered in the computation of the steel bar ratio.

The total volume of the steel bars was converted to the

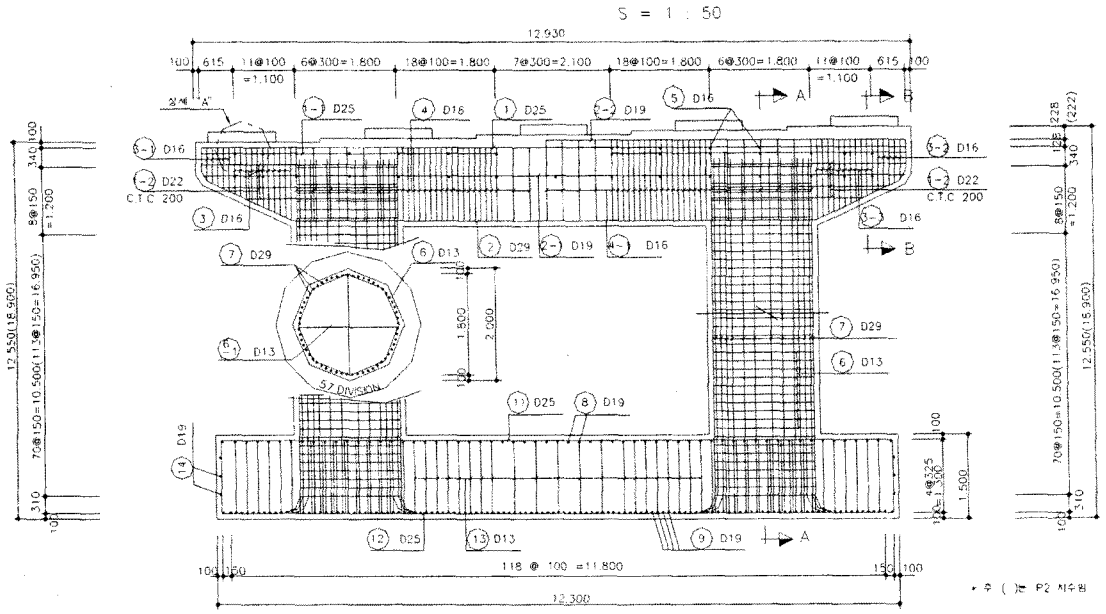

Fig. 3 Arrangement of reinforcing bar (front view).

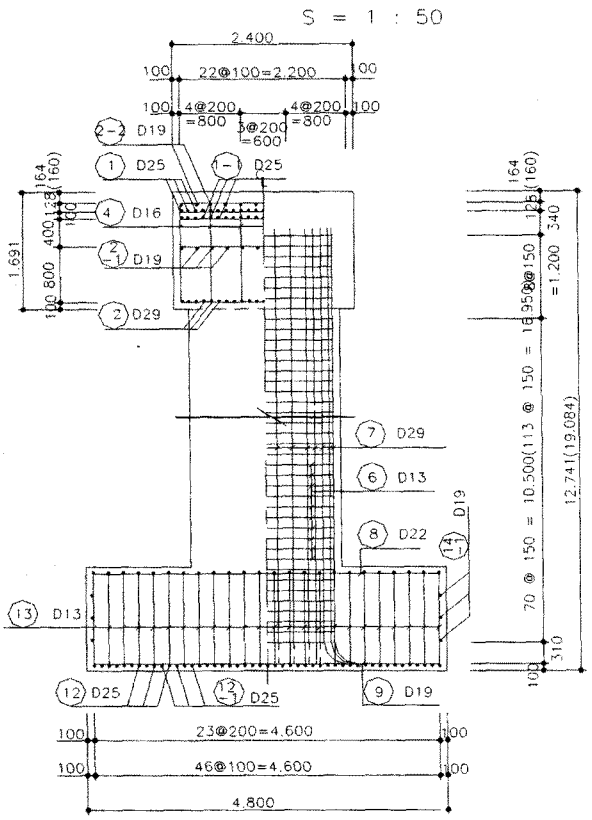

Fig. 4 Arrangement of reinforcing bar (side view).

thickness of the steel bars in two-dimensional plane in order to carry out the FEM by two-dimensional plane element. As seen in Figs. 3 and 4, because the main steel bars in the bridge axis direction and main steel bars in the perpendicular direction to the bridge axis were laid out in different direction but at the same location, they were modelled as one steel bar during the conversion to the two-dimensional element. Examining the main steel bars as an example of the conversion to two-dimensional element is provided. 46-D25 steel bars are laid out in bridge axis direction at 100 mm interval, and thus it has the thickness of $50.67 \times 46/440 = 5.30$ mm.

Here, 5.067 is the cross section of one steel bar, and 440 is the width of the floor plane. Because the 121-D19 steel bars are laid out in the direction perpendicular to the bridge axis at 100 mm interval, its thickness is computed to be $28.65 \times 121/1,210 = 2.87$ mm. Then, the thickness of main steel bars becomes $5.30 + 2.87 = 8.17$ mm finally for the conversion to two-dimensional plane. The same conversion process was applied to all steel bars including compressed steel bars, stirrups, etc. to determine the thickness of the steel bars converted to two-dimensional plane.

Fig. 5 shows the two-dimensional modelling of the structure composed of foundation base rock, concrete and steel bars for the finite element analysis. The structure modelled in this study is composed of concrete element, base rock element, and steel bar element. For all these elements of concrete, base rock, and steel bar, the two-dimensional (heat) conduction element with eight nodes was applied uniformly, and they were grouped by 50 mm intervals for each direction. Thus, 1,542 concrete elements, 2,460 base rock elements, and 472 steel bar elements were used and analyzed in this study.

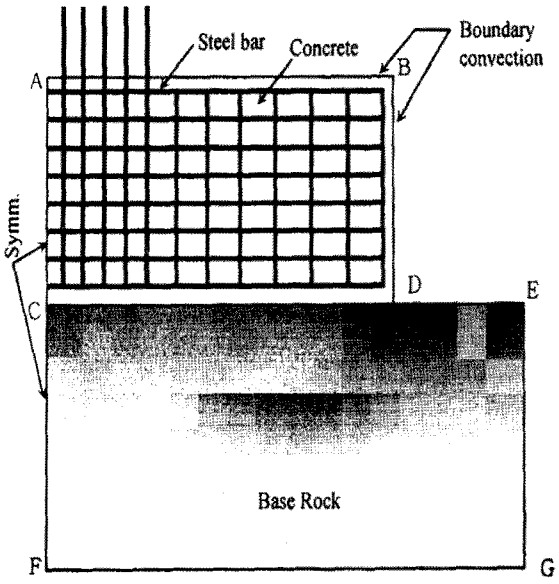

Fig. 5 Finite element model.

3.2.3 Initial condition and boundary condition

The initial condition for the analysis of hydration heat is the temperature of unhardened concrete at the time of concrete placement, the temperature of each material, the temperature of atmospheric air, etc. For the analysis, the temperature of the concrete at the time of concrete placement and the initial temperature of the steel bars were assumed to be 20°C uniformly. Moreover, the initial temperature of the base rock, to which the foundation is placed and laid out and the atmospheric temperature were assumed to be 10°C and 17°C, respectively.

The boundary condition is defined by the thermal property of the surface of the structure, i.e. the heat convectivity, which indicates the heat conductivity of any material and atmospheric air. In Fig. 5, the upper side (AB) was set to be the status of complete exposure to the atmospheric air from the time of initial placement of the concrete to the compete hardening of the concrete, and the side (BD) was to be exposed to the atmospheric air after 7 days (168 hrs) of the concrete form installed at the time of the concrete placement. Other symmetric sides and the surface of the base rock were assumed to be in adiabatic condition with no heat conduction. Thus, the coefficient of heat conductivity for the upper side (AB) was set to be 50.21 kJ/m^{2}hr°C, and that of the side (BD) was set at 20.92 kJ/m^{2}hr°C for the seven days of concrete form and was assumed to be equal to the heat convectivity with the outside air as the same as the upper side under the assumption of the removal of the concrete form after seven days thereafter. Additionally, because the concrete placement of the compressed steel bars in the foundation of the bridge column was carried out while being exposed to the outside, it was modelled with the condition of being exposed to the air, and its heat convectivity with the outside air was set at 1,372.35 kJ/m^{2}hr.

4. Analysis and discussion of the experimental result

4.1 Pattern of propagation of thermal (heat) flow

Fig. 6 shows the thermal vector flow as obtained by finite

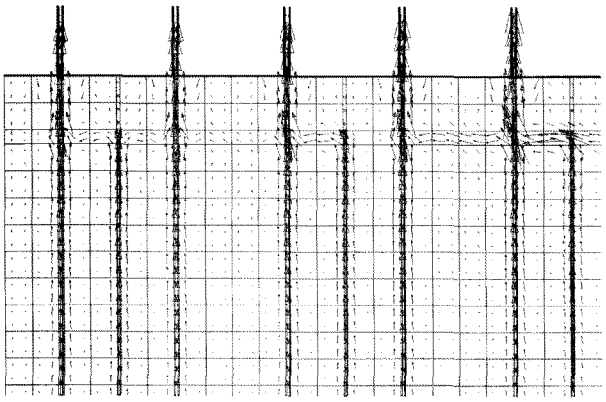

Fig. 6 Thermal vector flow.

element analysis. In Fig. 6, the length of the arrow represents the relative vector and confirms that the heat flow of the steel bar is a lot faster than that of concrete. This indicates that the steel bars transmit a lot more heat calorie compared to concrete in a given time period, and the thermal distribution of the overall structure shows a clear difference between the cases of considering steel bars and ignoring them. Additionally, the heat release to the outside can not be ignored also because considerable heat is released through the steel bars when we consider the influence of steel bars. Thus, it is deemed that steel bars function significantly in reducing the maximum temperature inside the steel-bar reinforced concrete structure.

4.2 Temperature distribution by steel bar ratio (content)

Fig. 7 shows temperature distribution after 48 hours for each steel bar ratio obtained by the finite element analysis. The maximum temperature was observed at 48 hours for all steel bar ratios, and the maximum temperature at the center was measured at 55.0°C when the influence of the steel bar was not considered (steel bar ratio of zero). As the steel bar ratio increased to 1.4%, 1.6%, and 1.8%, the maximum temperature at the center increased to 52.5°C, 50.1°C, and 47.2°C, respectively. The maximum temperature occurred at the center as expected and observed from the temperature distribution, and as it moved from the center to the outside surface, a distribution of a contour line of lower temperature was observed.

The model of steel bar ratio of zero (the case of not considering the influence of steel bar) showed a proportional decrease in temperature as it moved to the outside. This is a typical temperature distribution occurring due to the low heat conductivity of concrete, reflecting that the speed of heat calorie transmission from the inside to the outside is lower than the heat calorie released to the outside. On the other hand, the temperature distribution of the concrete reinforced by steel bar (the case of considering the effect of steel bar) shows a characteristic behavior of severe curve at the location of embedded steel bars. This is because the steel bars transmit heat faster than the concrete around them. Thus, the temperature around the steel bars shows the distribution of lower temperature, and this curve is more conspicuous as the steel bar ratio increases. Thus, we can see that the maximum temperature at the center decreases as the steel bar ratio increases. Additionally, after 48 hours when the maximum temperature was observed, the temperature at the center decreased with time. At the end, the temperature converged to the temperature at the time of initial concrete placement and outside air temperature. The distribution of temperature around the compressed steel bars embedded in the bridge pier column, which is exposed to the outside, showed a lower temperature than the temperature distribution around the stirrups embedded at the foundation. This is construed by the reasoning that the compressed steel bars in the bridge column is directly exposed to outside air, while the stirrups are covered with the concrete at the depth of the covering concrete, to make it more conducive to heat transmission. Thus, it is expected that the influence of steel bars will vary in accordance with the type of the structure.

The size of bridge pier foundation member considered in this study is relatively smaller than the foundation member of a large bridge. Nonetheless, since the height of mass concrete member of large size is relatively tall, the concrete is placed in several proportions. At this time of mass concrete placement, the height (amount) of the concrete placement in a given time us determined in consideration of the magnitude of heat of hydration. In this case, because all steel bars laid out at the foundation in perpendicular

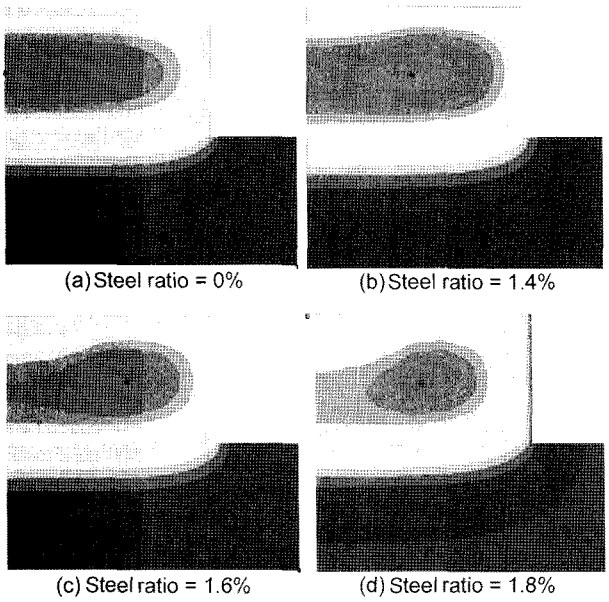

Fig. 7 Temperature distribution after 48 hours.

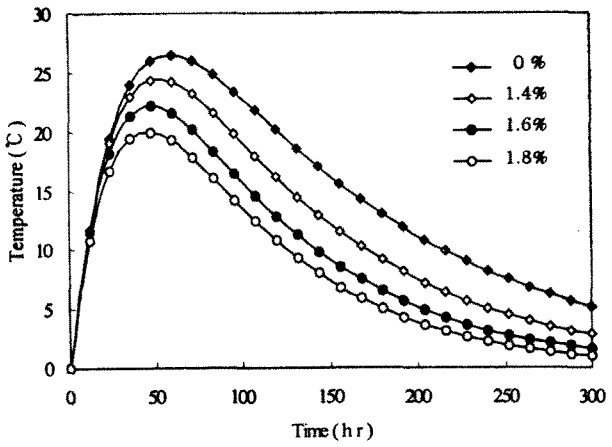

Fig. 8 Temperature difference between center and surface of concrete.

direction are exposed to the outside during the concrete placement, the heat transmission to the outside through the steel bars will be easier, and the maximum temperature inside the concrete will decrease proportionally.

Fig. 8 shows the temperature difference between the center and the surface of the concrete with time passage. The maximum difference in temperature between the center and the surface in case of not considering the influence of steel bars (steel bar ratio of zero) and the case of 1.8% steel bar ratio by volume is 26.5°C and 20.0°C. Thus, when the steel bar ratio is increased from zero percent (no steel bar) to 1.8% by volume, it decreased the maximum temperature difference between the center and the surface of the concrete by 32.5%.

4.3 Stress distribution by steel ratio

The analysis of stress on the concrete was carried out by using the temperature distribution obtained from the result of temperature analysis as the input for the load.

Fig. 9 shows the distribution of tensile stress at the surface of the concrete. The maximum tensile stress at the surface of the cross section with no reinforcing steel bar was measured at 5.77 MPa after 60 hours. Additionally, the maximum tensile stress for the cases of steel bar ratios of 1.4%, 1.6%, and 1.8% was measured at 5.67 MPa, 5.44 MPa, and 5.20 MPa, respectively. When the cracking stress is computed to be $f_r = 0.63(f_{ck})^{1/2}$ pursuant to the Concrete Standard Specifications[6] and 25 MPa is substituted for f_{ck}, the cracking stress becomes 3.15 MPa. Thus, cracking due to temperature (heat) is expected.

Because the maximum temperature difference between the center and the surface of the concrete is drastically reduced by the increase in steel bar ratio, the confinement stress inside the concrete decreases. Thus, it is construed that the maximum tensile stress at the surface of the concrete is reduced as the result. Comparing the analysis of concrete with 1.8% steel bar against that with no steel bar, the former resulted in the reduction of tensile stress by 10%. As the steel bar ratio increases, the stress reduction also becomes greater. Considering that the steel bar ratio of typical structures is in the range of 2.0~2.4%, it is deemed that bigger reduction of the tensile stress is possible.

4.4 Thermal cracking

The Concrete Standard Specifications[7] stipulates to lay out thermal steel bars to control for thermal cracking due to the thermal stress from the heat of hydration. The cracking index to determine the degree of thermal cracking can be expressed as follows.

$$I_{cr}(t) = \frac{f_{sp}(t)}{f_t(t)} \quad (4)$$

where, $f_t(t)$: maximum thermal stress at t days of age
$f_{sp}(t)$: tensile strength at t days of age

The analysis result of substituting thermal stress and tensile strength to eq. (4) above indicated that the thermal cracking index decreased by 11.0% for the case of steel bar ratio of 1.8%. Fig. 10 depicts a graph to examine the thermal cracking index and the probability of the occurrence of thermal cracking from the Concrete Standard Specifications,[6] and the reduction in thermal

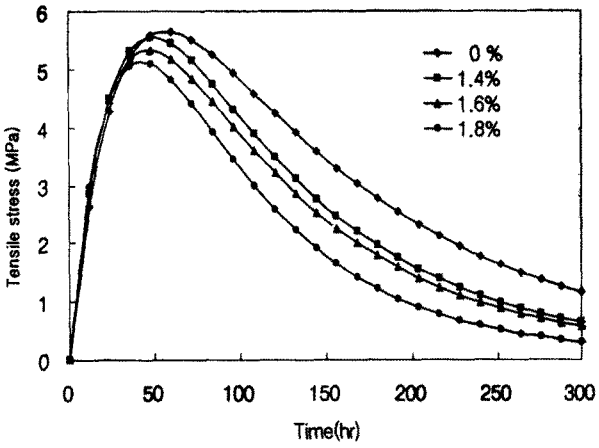

Fig. 9 Tensile stress distribution at surface.

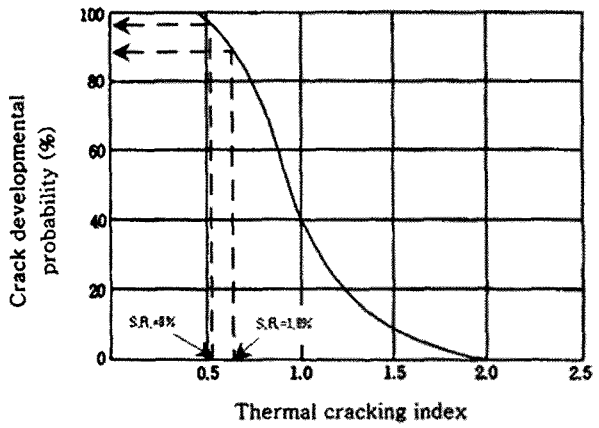

Fig. 10 Thermal cracking index vs. developmental probability.

cracking index by 11.0% indicates about 10.0% reduction in the probability of the occurrence of cracking. Although it is difficult to determine the reduced amount of thermal steel bar directly from this 10.0% reduction in the probability of the occurrence of cracking, about 10% reduction in the thermal steel bar along with the reduction in the maximum crack width can be expected from the relationship between maximum crack width and thermal cracking index based on the Concrete Standard Specifications.[6]

5. Conclusion

This study examined the influence of steel bars reinforcing concrete structures on the dispersion and distribution of the heat calorie due to heat of hydration and the change in the thermal stress caused by it. For this research objective, two-dimensional finite element analysis on bridge pier foundation was carried out, and the model with gradually increasing steel bar ratio and the model with no steel bar were compared.

When the model with no steel bar and the model with steel bar ratio of 1.8% were compared, the maximum temperature difference between the center and the surface of the concrete structure was reduced by 32.5% due to the faster heat conductivity of the steel bar. Additionally, it was also confirmed that the degree of reduction in the maximum temperature difference between the center and the surface increased as the steel bar ratio increased. Moreover, it was found that the reduction in the temperature difference between the inside and outside of the

structure by 32.5% had the effect of reducing the tensile stress at the surface by approximately 10.0%. With this result, 11.0% reduction in the thermal cracking index and about 15.0% reduction in the probability of the occurrence of cracking were expected based on the suggestion of the Concrete Standard Specifications.[6] In return, the reduction in the quantity of thermal steel for the control of thermal cracking could be expected. Additionally, if analysis and experimental studies on various types of structures are carried out in the future, it is well anticipated that more rational design and construction will be possible with the analysis of heat of hydration and the prediction of thermal stress on such structures reinforced with steel bars.

Acknowledgements

This research has been supported by the research fund of Dongguk University. The authors express their sincere appreciation for it.

References

1. Kang, S. H., Chung, C. H., Jeong, H. J., Lee, Y. H., and Park, C. L., "A Study on the Evaluation of Thermal Stress of Massive Concrete Structure", *Journal of Korea Concrete Institute*, Vol.7, No.2, 1995, pp.126~135.

2. Kim, E. K., Kim, L. H., and Shin, C. B., "Development of Temperature-analysis Program for Mass Concrete Using Finite Element Method", *Journal of Korea Concrete Institute*, Vol.7, No.6, 1995, pp.167~175.

3. Kim, J. K. and Yang, E. I., "Factors for Hydration Heat and Thermal Stress in Mass Concrete", *Journal of Korea Concrete Institute*, Vol.9, No.3, 1997, pp.15~23.

4. Kim, J. K., Kim, K. H., and Yang, J. K., "Thermal Analysis of the Heat of Hydration in Concrete with Considering Heat Reduction Techniques", *Journal of Korea Concrete Institute*, Vol.7, No.6, 1995, pp.176~185.

5. Oh, B. H. and Paik, S. W., "Temperature Analysis and Crack Control of Large Scale Massive Concrete Structures Due to Hydration Heat", *Journal of Korea Concrete Institute*, Vol. 7, No. 1, 1995, pp.97~108.

6. Korea Concrete Institute, "Concrete Standard Specifications", Korea Concrete Institute, 1999.

7. ADINA, "Theory and Application," ADINA, Vol.1, 2001.